International Journal of Modern Physics A

Statistical properties of undulator radiation*

Sergei Nagaitsev†

Fermilab
Batavia, IL 60510, USA
nsergei@fnal.gov

Giulio Stancari

Fermilab
Batavia, IL 60510, USA
stancari@fnal.gov

Ihar Lobach

Argonne National Laboratory
Lemont, IL 60439, USA
ilobach@anl.gov

Received Day Month Year
Revised Day Month Year

Most often, noise is encountered in a negative context and is considered something that needs to be minimized. However, there are multiple examples where noise is used as a non-invasive probe into the parameters of a certain system, and even to measure fundamental constants. In this paper we describe two experiments, which were carried out to study the statistical properties of undulator radiation in the Integrable Optics Test Accelerator (IOTA) storage ring at Fermilab. The first experiment studied the turn-to-turn fluctuations in the power of the radiation generated by an electron bunch. The magnitude of these fluctuations depends on the 6D phase-space distribution of the electron bunch. In IOTA, we demonstrated that this effect can be used to measure some electron bunch parameters, small transverse emittances in particular. In the second experiment, a single electron was stored in the ring, emitting a photon only once per several hundred turns. In this regime, any classical interference-related collective effects were eliminated, and the quantum fluctuations could be studied in detail to search for possible deviations from the expected Poissonian photon statistics. In addition, the photocount arrival times were used to track the longitudinal motion of a single electron and to compare it with simulations. This allowed us to determine several dynamical parameters of the storage ring such as the rf cavity phase jitter and the dependence of the synchrotron motion period on amplitude.

Keywords: Fluctuations, statistical properties.

*This research is supported by Fermi Research Alliance, LLC under Contract No. DE-AC02-07CH11359 with the U.S. Department of Energy and by the University of Chicago.
†Also at the University of Chicago

1. Introduction

There exist multiple examples where fluctuations and noise are used as a non-invasive probe into the parameters of a certain system, and even to measure fundamental constants. Examples include the determination of the Boltzmann constant k_B by the thermal noise in an electrical conductor[1] and the measurement of the elementary charge e by the shot noise of the electric current in a vacuum tube.[2] In fact, the latter effect is also relevant to accelerators and storage rings, where it is known as Schottky noise[3] due to the finite number of charge carriers in the beam, as described by Schottky.[4] Many beam parameters, such as the momentum spread, the number of particles and even transverse rms emittances, are imprinted into the power spectrum of Schottky noise. It is often used in beam diagnostics[5–7] and beam cooling.[3] Swapan Chattopadhyay has described[8,9] many fundamental aspects of fluctuations and coherence in charged-particle beams in storage rings. In this paper we extend his description to spontaneous synchrotron radiation, emitted by charged particles in a ring.

In our experiments[10–13] with an electron bunch we showed that turn-to-turn fluctuations $\mathrm{var}(\mathcal{N})$ of the number of detected undulator radiation photons per turn $\mathcal{N}$ have two contributions: (1) a Poissonian contribution equal to $\langle\mathcal{N}\rangle$, due to the discrete quantum nature of light, and (2) a collective contribution $\propto \langle\mathcal{N}\rangle^2$, related to the interference between the fields generated by the electrons in the bunch. We also eliminated the collective contribution by studying a single electron, circulating in the Integrable Optics Test Accelerator (IOTA) storage ring at Fermilab in order to thoroughly study the quantum fluctuations and verify that they follow the Poissonian photostatistics $\mathrm{var}(\mathcal{N}) = \langle\mathcal{N}\rangle$, predicted by.[14–17] This research is motivated by the surprising observation of sub-Poissonian photostatistics ($\mathrm{var}(\mathcal{N}) < \langle\mathcal{N}\rangle$) in synchrotron radiation reported in Ref.[18] in a similar experiment setting. In addition, we use the recorded detection times to study the synchrotron motion of a single electron in IOTA,[19] similar to previous experiments in Novosibirsk.[20,21]

2. Radiation fluctuations

Synchrotron radiation is generated by individual electrons in the beam. Hence, Schottky noise in the beam current must pass on to the synchrotron radiation power in some way. Therefore, one could assume that the synchrotron radiation power noise may carry information about beam parameters as well. This assumption is, in fact, correct. Three decades ago, Ref.[22] reported the results of an experimental study into statistical properties of wiggler radiation in a storage ring. It was noted that the magnitude of turn-to-turn intensity fluctuations depends on the dimensions of the electron bunch. The potential in beam instrumentation was soon realized[23] and a number of papers followed. However, to this day, mostly measurements of a bunch length via these fluctuations were discussed.[24–26] Only Ref.[27] reported an order-of-magnitude measurement of a transverse emittance. In our previous publications,[10] we described a new fluctuations-based technique for an absolute measurement of a transverse emittance. There are no free parameters in our equations, nor is a calibration required. However, the transverse and longitudinal focusing functions of the storage ring are assumed to be known. This technique was successfully tested at the Integrable Optics Test Accelerator (IOTA) storage ring at Fermilab.[28] For a beam with approximately equal and relatively large transverse rms emittances, the results agreed with conventional visible synchrotron light monitors (SLMs).[29] Then, in a different regime, we measured a much smaller vertical emittance of a flat beam, unresolvable by our SLMs. These emittance measurements agreed with estimates, based on the beam lifetime. The fluctuations var($\mathcal{N}$) are shown in Figs. 1(a),(b) with a statistical error of 2.7×10^6 (at all beam currents), which was determined with an independent test light source.[11] The numerical solution of Eq. (1) for the unknown emittance, with M from Eq. (2) of Ref.,[11] was performed on the Midway2 cluster at the University of Chicago Research Computing Center. The results for the measured emittances are shown in Figs. 1(c),(d) (red points). The error bars correspond to the statistical error of the fluctuations measurement. Apart from this statistical error there is also a systematic error due to the 1 MeV uncertainty on the beam energy (from 10 nm at lower beam currents to 14 nm at higher currents).

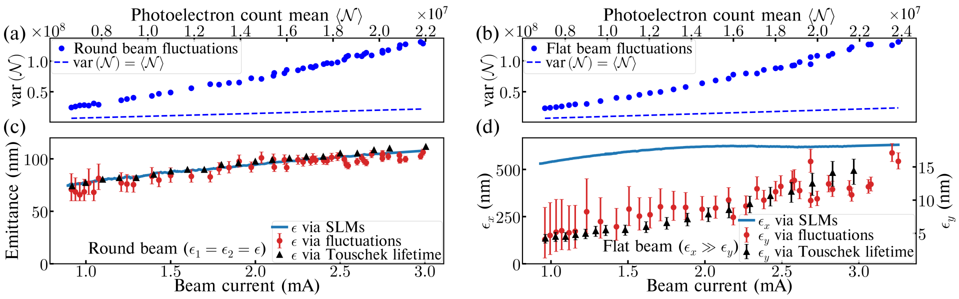

Fig. 1. Panels (a) and (b) show the measured fluctuations for the round and flat beams, respectively. The statistical error of each point is 2.7×10^6 (not shown). (c) The round-beam mode emittance ϵ, determined via SLMs, via undulator radiation fluctuations, and via Touschek lifetime, assuming the effective momentum acceptance 2.0×10^{-3}. (d) The flat-beam horizontal emittance measurement via SLMs (left scale), the vertical emittance measurement via fluctuations and via Touschek lifetime (right scale). The SLMs had a monitor-to-monitor spread of ± 8 nm (round beam) and ± 50 nm (horizontal emittance of flat beam); these error bars are not shown. All emittances are rms, unnormalized.

To understand the nature of these fluctuations, let us assume that we have a detector that can measure the number of detected synchrotron radiation photons $\mathcal{N}$ at each revolution in a storage ring. Then, according to,[12,17,22,30] the variance of this number is

$$\mathrm{var}(\mathcal{N}) = \left\langle \left(\mathcal{N} - \langle\mathcal{N}\rangle\right)^2 \right\rangle = \langle\mathcal{N}\rangle + \frac{1}{M}\langle\mathcal{N}\rangle^2 , \tag{1}$$

where the linear term represents the photon shot noise, related to the quantum discrete nature of light. This effect would exist even if there was only one electron, circulating in the ring. Indeed, the electron would radiate photons with a Poisson distribution.[14–16] The quadratic term in Eq. (1) corresponds to the interference of fields, radiated by different electrons. Changes in relative electron positions and velocities, inside the bunch, result in fluctuations of the radiation power and, consequently, of the number of detected photons. In a storage ring, the effect arises from betatron and synchrotron motion, from radiation induced diffusion, etc. The dependence of var($\mathcal{N}$) on the 6D phase-space distribution of the electron bunch is introduced through the parameter M, which is conventionally called the number of coherent modes.[12,22,30] In addition to bunch parameters, M depends on the specific spectral-angular distribution of the radiation, on the angular aperture, and on the detection efficiency (as a function of wavelength). We derived an equation for M [Eq. (2) of Ref.[11]] for a Gaussian transverse beam profile and an arbitrary longitudinal bunch density distribution $\rho(z)$ (normalized), assuming an rms bunch length much longer than the radiation wavelength. In our analysis, M is calculated by this equation numerically, using our computer code,[31] as a function of transverse emittances ϵ_x and ϵ_y, the rms momentum spread σ_p, and the effective bunch length, $\sigma_z^{\mathrm{eff}} = 1/(2\sqrt{\pi}\int\rho^2(z)\,\mathrm{d}z)$, equal to the rms bunch length, σ_z, for a Gaussian distribution.

For illustration purposes, let us assume a Gaussian spectral-angular distribution for the number of detected photons $\mathcal{N}$, namely,

$$\frac{\mathrm{d}^3\mathcal{N}}{\mathrm{d}k\mathrm{d}\theta_x\mathrm{d}\theta_y} = C\exp\left[-\frac{(k-k_0)^2}{2\sigma_k^2} - \frac{\theta_x^2}{2\sigma_{\theta_x}^2} - \frac{\theta_y^2}{2\sigma_{\theta_y}^2}\right], \tag{2}$$

where k is the magnitude of the wave vector, θ_x and θ_y represent the horizontal and vertical angles of the direction of the radiation in the paraxial approximation, k_0 refers to the center of the radiation spectrum, σ_k is the spectral rms width, σ_{θ_x} and σ_{θ_y} are the angular rms radiation sizes, C is a constant. Then[11,24]

$$M = \sqrt{1+4\sigma_k^2\sigma_z^2}\sqrt{1+4k_0^2\sigma_{\theta_x}^2\sigma_x^2}\sqrt{1+4k_0^2\sigma_{\theta_y}^2\sigma_y^2}, \tag{3}$$

where σ_x, σ_y, σ_z are the rms sizes (determined by beam emittances) of a Gaussian electron bunch. In addition, it is assumed that the radiation is longitudinally incoherent $k_0\sigma_z \gg 1$ and that the radiation bandwidth is very narrow $\sigma_k \ll 1/(\sigma_x\sigma_{\theta_x})$, $\sigma_k \ll 1/(\sigma_y\sigma_{\theta_y})$. In general, the distribution parameters k_0, σ_k, σ_{θ_x}, σ_{θ_y} are determined by both the properties of the emitted synchrotron radiation and by the properties of the detecting system (angular aperture, detection efficiency). In Eq. (3), the beam divergence is neglected and M depends on σ_x and σ_y, as opposed to a more general result [Eq. (2) of Ref.[11]], where it depends on ϵ_x and ϵ_y.

3. Photostatistics for a single electron

To eliminate the collective contribution to the fluctuations, var($\mathcal{N}$), experiments were performed with a single electron, circulating in IOTA with a revolution period of 133 ns and an energy of 96.4 MeV. The undulator parameter is $K_{\mathrm{u}} = 1.0$ with the

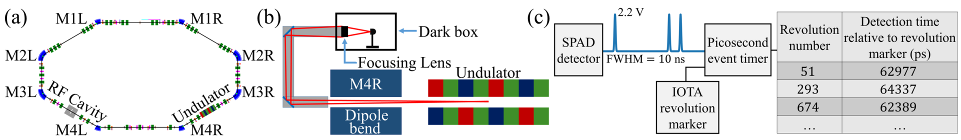

Fig. 2. (a) Layout of IOTA, electrons circulate clockwise. (b) Light path from the undulator to the detector (not to scale). (c) Block diagram of the data acquisition system.

number of periods $N_\mathrm{u} = 10.5$ and the period length $\lambda_\mathrm{u} = 5.5\,\mathrm{cm}$. The wavelength of the fundamental was $\lambda_1 = \lambda_\mathrm{u}(1 + K_\mathrm{u}^2/2)/(2\gamma^2) = 1.16\,\mu\mathrm{m}$, where $\gamma = 188.6$ is the Lorentz factor. The second harmonic was in the visible wavelength range. We used a Single Photon Avalanche Diode (SPAD)[32] as a detector, which was mostly sensitive to the visible light with detection efficiency of up to 65 %. Two edge-pass filters were used to only collect the radiation between 550 nm and 800 nm. The radiation was focused on the sensitive area of the detector ($\varnothing 180\,\mu\mathrm{m}$) by a single focusing lens with a focal distance of 180 mm, see Figs. 2(a),(b). The radiation was collected in a large angle $> 1/\gamma$. The SPAD detector produced a 10-ns-long TTL pulse at each detection event. Its dead time (20 ns) was shorter than the IOTA revolution period (133 ns). Our data acquisition system [Fig. 2(c)] allowed us to record the revolution number and the arrival time relative to the IOTA revolution marker for each detection event for as long as 1 minute at a time.

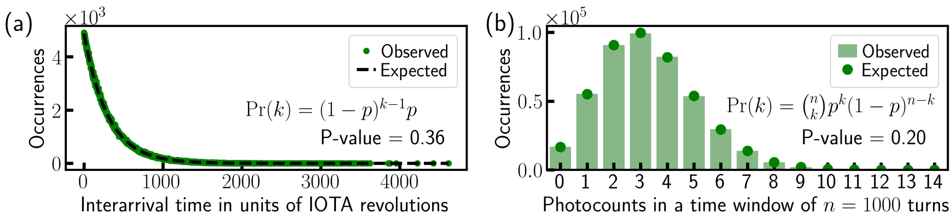

Fig. 3. (a) The measured distribution of interarrival times between the photocounts and a fit by a geometric distribution. (b) The measured distribution of the number of photocounts in a time window equal to $n = 1000$ IOTA revolutions and a fit by a binomial distribution.

In the optimal focusing, the measured photocount rate was 24.7 kHz, or one photocount per 304 revolutions in IOTA (on average). The dark count rate of the SPAD detector was 108 Hz. In addition, we used a 5-ns-long gate around the expected detection arrival time, which allowed us to reduce the effective dark count rate to 4.0 Hz.

Before any analysis of the photostatistics, it was important to realize that the SPAD detector is binary. It produces the same type of pulses (TTL, 10-ns-long) no matter how many photons are detected per one pass. The collected turn-by-turn data can be represented as a sequence of zeros and ones only. Therefore, we had to alter our original expectation of Poissonian photostatistics to a sequence of

Bernoulli trials, i.e., there is a probability p of a detection at every revolution, and a probability $(1-p)$ of no detection. In our case, $p = (3.29 \pm 0.02) \times 10^{-3}$. Figure 3 illustrates the comparison between the expectation (for a sequence of Bernoulli trials) and the measurement for (a) the distribution of interarrival times and for (b) the distribution of the number of photocounts in a certain time window. In both cases, the χ^2 goodness-of-fit test [33, p. 637] results in a P-value [33, p. 140] above the conventional 0.05 threshold. This means that the null hypothesis (exponential or binomial distribution, respectively) cannot be rejected.

Some measurements were carried out with an upgraded setup consisting of two SPAD detectors separated by a beam splitter.[34] In this case, the photon number resolution was improved, since there were three possible outcomes for each pass: 0, 1, or 2 detection events. Still, so far we have not observed anything unusual. There was no statistically significant correlation or anticorrelation in the two detectors.

4. Synchrotron motion

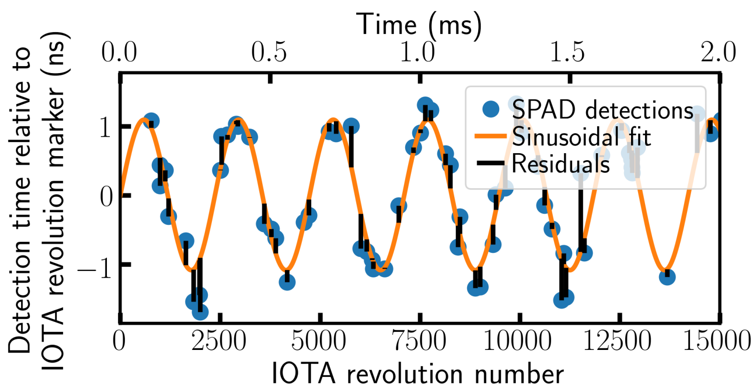

Fig. 4. Illustration of the fitting procedure for determination of the synchrotron motion period and amplitude.

Figure 4 illustrates the detection time relative to the IOTA revolution marker as a function of the IOTA revolution number. The observed sinusoidal motion is, in fact, the synchrotron motion of a single electron. The deviations from the sinusoidal fit are due to the time resolution of the SPAD detector (about 0.4 ns rms). On a larger time scale, the amplitude of the synchrotron motion grows and decreases randomly due to the quantum excitation and radiation damping.

We decided to compare the measured arrival times with a simulation of the synchrotron motion. In our simulation[35] we use the following transformation of the relative energy deviation δ_i and the rf phase ϕ_i of a single electron from turn i to

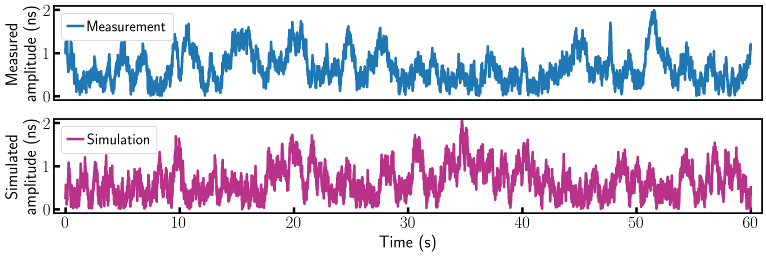

Fig. 5. Amplitude of the synchrotron motion of a single electron as a function of time. In the simulation, the rms rf phase jitter is $\sigma_\xi = 6.0 \times 10^{-5}$ rad.

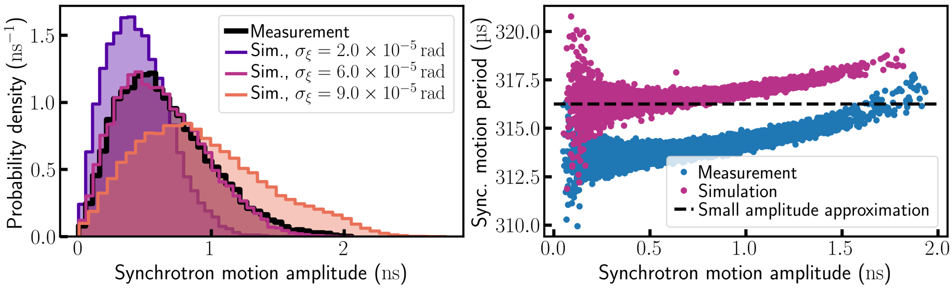

Fig. 6. Panel (a) shows the comparison of the measured and simulated distributions of the synchrotron motion amplitude. The best agreement is achieved at the rms rf phase jitter $\sigma_\xi = 6.0 \times 10^{-5}$ rad. Panel (b) shows the synchrotron motion period as a function of the synchrotron motion amplitude.

turn $i + 1$,

$$\delta_{i+1} = \delta_i + \frac{eV_0}{E_0}(\sin\phi_i - \sin\phi_s) - \frac{\langle U \rangle \mathcal{J}_E}{E_0}\delta_i - \frac{U_i - \langle U \rangle}{\beta^2 E_0}, \tag{4}$$

$$\phi_{i+1} = \phi_i - 2\pi q \eta_s \delta_{i+1} + \xi_i, \tag{5}$$

where e is the electron charge, $E_0 = \gamma m_e c^2 = 96.4\,\mathrm{MeV}$, m_e is the electron mass, c is the speed of light, $\beta = \sqrt{1 - 1/\gamma^2}$ is the relativistic velocity parameter, $V_0 = 380\,\mathrm{V}$ is the rf voltage amplitude, $q = 4$ is the rf harmonic number, $\eta_s = \alpha_c - 1/\gamma^2 = 0.070\,83$ is the phase slip factor (variation of η due to variation of γ is negligible), $\alpha_c = 0.070\,86$ is the momentum compaction factor, $\mathcal{J}_E = 2.64$ is the longitudinal damping partition number [36, p. 445], U_i is the radiation energy loss at ith turn, ξ_i is the rf cavity phase jitter at the ith turn. We model ξ_i as a random variable following a normal distribution with a standard deviation σ_ξ. We refer the reader to [36, Eq. (3.28)] for the symplectic part of the transformation. The derivation of the synchrotron damping term, $-\langle U \rangle \mathcal{J}_E \delta_i / E_0$, is described in [36, pp. 438–445]. The quantum excitation term, $-(U_i - \langle U \rangle)/(\beta^2 E_0)$, is considered in.[37] The energy kick at the synchronous phase ϕ_s compensates for the average energy loss due to the synchrotron radiation, i.e., $eV_0 \sin\phi_s = \langle U \rangle$. The average emitted energy per turn in an isomagnetic ring is [36, pp. 434–435] $\langle U\rangle = 8\pi\alpha\gamma u_c/9 = 10.9\,\text{eV}$, where α is the fine-structure constant, $u_c = 3\hbar c\gamma^3/(2\rho) = 2.8\,\text{eV}$ is the critical energy [37, Eq. (11)], $\rho = 70\,\text{cm}$ is the electron trajectory radius in the dipole magnets, $\hbar$ is the reduced Plank constant. The isomagnetic ring approximation works well in IOTA, the radiation in the undulator is negligible compared to the bending magnets. The average number of photons emitted per turn in an isomagnetic ring is[37] $\langle\mathcal{N}\rangle = 5\pi\alpha\gamma/\sqrt{3} = 12.5$. To simulate the number of emitted photons at ith revolution, we use a Poisson random number generator with the expectation value $\langle\mathcal{N}\rangle = 12.5$. To simulate the energies of these photons, we use the Monte Carlo generator described in Ref.[37] The sum of these energies gives U_i.

Using our computer code we can generate the data points as in Fig. 4 for a long interval of time, e.g., 1 minute. By fitting the data with short pieces of sinusoidal curves (as in Fig. 4) one can plot the synchrotron motion amplitude as a function of time, see Fig. 5. We cannot compare the measurement and the simulation in this way directly, because it is a stochastic process. However, we can compare the distributions of the synchrotron motion amplitudes. Figure 6(a) illustrates such a comparison, where the simulation results are presented at three different values of the rms rf phase jitter σ_ξ. We can conclude that in IOTA $\sigma_\xi \approx 6.0\times10^{-5}\,\text{rad}$. We considered more values of σ_ξ than illustrated in Fig. 6(a). Further, using the same piecewise sinusoidal fit we can plot the synchrotron motion period as a function of the synchrotron motion amplitude, see Fig. 6(b). Every point in Fig. 6(b) is calculated from a 25-ms-long interval of time. The measured and the simulated synchrotron motion periods agree rather well, which shows that we understand the parameters of the IOTA ring well.

5. Summary

Synchrotron light sources and free-electron lasers, thanks to their brightness, spectral content, and temporal structure, are some of the best laboratory-based sources of X-ray radiation for the study of physical processes, chemical reactions, biological structures, and the properties of materials.

The role and relevance of the statistical and coherence properties of synchrotron radiation is well recognized. It is common to separate the description into quantum and classical regimes. For example, in the past few decades, substantial progress has been made in understanding the classical properties of spontaneous radiation in various magnetic insertion devices, such as bending magnets, wigglers and undulators. In fact, the predictions of classical electrodynamics for the average characteristics of synchrotron radiation are supported by countless observations at synchrotron radiation facilities around the world. On the other hand, the statistical properties of synchrotron radiation have not been studied to the same level of detail yet.

Our studies tackle several questions in our understanding of the turn-to-turn fluctuations in synchrotron radiation in a storage ring, both theoretically and experimentally. We proposed how to close the gap between the descriptions of classical and quantum fluctuations, carried out a series of thorough experimental measurements, and developed new applications, based on the improved understanding.

6. Acknowledgments

This paper is in honor of Swapan Chattopadhyay, who vigorously supported and encouraged our science program at IOTA and who has made fundamental contributions to the theory of fluctuations in charged-particle beams.[8,9]

We are grateful for the support of the University of Chicago Research Computing Center for assistance with the calculations carried out in this work.

References

1. J. B. Johnson, *Phys. Rev.* **32**, 97 (1928).
2. A. W. Hull and N. Williams, *Phys. Rev.* **25**, 147 (1925).
3. S. van der Meer, *Nobel Lecture* (Dec 1984).
4. W. Schottky, *Annalen der Physik* **362**, 541 (1918), doi:10.1002/andp.19183622304.
5. D. Boussard, *Schottky noise and beam transfer function diagnostics*, Tech. Rep. CERN-SPS-86-11-ARF (May 1986).
6. S. van der Meer, Diagnostics with Schottky noise, in *Frontiers of Particle Beams; Observation, Diagnosis and Correction*, (Springer, 1989) pp. 423–433.
7. F. Caspers, J. M. Jimenez, O. R. Jones, T. Kroyer, C. Vuitton, T. W. Hamerla, A. Jansson, J. Misek, R. J. Pasquinelli, P. Seifrid *et al.*, The 4.8 GHz LHC Schottky pick-up system, in *2007 IEEE Particle Accelerator Conference (PAC)*, (2007), pp. 4174–4176.
8. S. Chattopadhyay, *Some fundamental aspects of fluctuations and coherence in charged-particle beams in storage rings* (CERN, Geneva, 1984).
9. S. Chattopadhyay, Stochastic cooling of bunched beams from fluctuation and kinetic theory `https://www.osti.gov/biblio/5045055`, (1982).
10. I. Lobach, S. Nagaitsev, V. Lebedev, A. Romanov, G. Stancari, A. Valishev, A. Halavanau, Z. Huang and K.-J. Kim, *Phys. Rev. Lett.* **126**, 134802 (4 2021), doi: 10.1103/PhysRevLett.126.134802.
11. I. Lobach, S. Nagaitsev, V. Lebedev, A. Romanov, G. Stancari, A. Valishev, A. Halavanau, Z. Huang and K.-J. Kim, *Phys. Rev. Accel. Beams* **24**, 040701 (4 2021), doi: 10.1103/PhysRevAccelBeams.24.040701.
12. I. Lobach, V. Lebedev, S. Nagaitsev, A. Romanov, G. Stancari, A. Valishev, A. Halavanau, Z. Huang and K.-J. Kim, *Phys. Rev. Accel. Beams* **23**, 090703 (Sep 2020), doi:10.1103/PhysRevAccelBeams.23.090703.
13. I. Lobach, A. Halavanau, Z. Huang, K. Kim, V. Lebedev, S. Nagaitsev, A. Romanov, G. Stancari and A. Valishev, Transverse Beam Emittance Measurement by Undulator Radiation Power Noise, in *Proc. IBIC'21*, International Beam Instrumentation Conference (JACoW Publishing, Geneva, Switzerland, 10 2021), pp. 167–167. https://doi.org/10.18429/JACoW-IBIC2021-TUOA03.
14. R. J. Glauber, *Phys. Rev.* **84**, 395 (1951).
15. R. J. Glauber, *Phys. Rev.* **131**, 2766 (1963).
16. R. J. Glauber, *Phys. Rev.* **130**, 2529 (1963).
17. J.-W. Park, An investigation of possible non-standard photon statistics in a free-electron laser, PhD thesis, University of Hawaii at Manoa (2019).
18. T. Chen and J. M. Madey, *Phys. Rev. Lett.* **86**, 5906 (2001).

19. I. Lobach, S. Nagaitsev, A. Romanov and G. Stancari, *Journal of Instrumentation* **17**, P02014 (Feb 2022), doi:10.1088/1748-0221/17/02/p02014.
20. A. Aleshaev, I. Pinayev, V. Popik, S. Serednyakov, T. Shaftan, A. Sokolov, N. Vinokurov and P. Vorobyov, *Nuclear Instruments and Methods in Physics Research Section A: Accelerators, Spectrometers, Detectors and Associated Equipment* **359**, 80 (1995), doi:https://doi.org/10.1016/0168-9002(96)88028-4, Proceedings of the 10th National Synchrotron Radiation Conference.
21. I. Pinayev, V. Popik, T. Shaftan, A. Sokolov, N. Vinokurov and P. Vorobyov, *Nuclear Instruments and Methods in Physics Research Section A: Accelerators, Spectrometers, Detectors and Associated Equipment* **341**, 17 (1994), doi:https://doi.org/10.1016/0168-9002(94)90308-5.
22. M. C. Teich, T. Tanabe, T. C. Marshall and J. Galayda, *Phys. Rev. Lett.* **65**, 3393 (1990).
23. M. S. Zolotorev and G. V. Stupakov, *Fluctuational interferometry for measurement of short pulses of incoherent radiation*, Tech. Rep. SLAC-PUB-7132, SLAC (Mar 1996).
24. F. Sannibale, G. Stupakov, M. Zolotorev, D. Filippetto and L. Jägerhofer, *Phys. Rev. ST Accel. Beams* **12**, 032801 (2009).
25. V. Sajaev, Measurement of bunch length using spectral analysis of incoherent radiation fluctuations, in *AIP Conf. Proc.*, (1) (AIP, 2004), pp. 73–87.
26. V. Sajaev, *Determination of longitudinal bunch profile using spectral fluctuations of incoherent radiation*, Report No ANL/ASD/CP-100935, Argonne National Laboratory (2000).
27. P. Catravas, W. Leemans, J. Wurtele, M. Zolotorev, M. Babzien, I. Ben-Zvi, Z. Segalov, X.-J. Wang and V. Yakimenko, *Phys. Rev. Lett.* **82**, 5261 (1999).
28. S. Antipov, D. Broemmelsiek, D. Bruhwiler, D. Edstrom, E. Harms, V. Lebedev, J. Leibfritz, S. Nagaitsev, C.-S. Park, H. Piekarz *et al.*, *J. Instrum.* **12**, T03002 (2017).
29. N. Kuklev, J. Jarvis, Y. Kim, A. Romanov, J. Santucci and G. Stancari, Synchrotron radiation beam diagnostics at IOTA — commissioning performance and upgrade efforts, in *Proc. 10th International Particle Accelerator Conference (IPAC'19), Melbourne, Australia, 19-24 May 2019*, International Particle Accelerator Conference (JACoW Publishing, Geneva, Switzerland, Jun. 2019), pp. 2732–2735. https://doi.org/10.18429/JACoW-IPAC2019-WEPGW103.
30. K.-J. Kim, Z. Huang and R. Lindberg, *Synchrotron radiation and free-electron lasers* (Cambridge University Press, 2017).
31. I. Lobach, The source code for calculation of fluctuations in wiggler radiation `https://github.com/IharLobach/fur`, (2020).
32. SPCM-AQRH
Single-Photon Counting Module `https://www.excelitas.com/product/spcm-aqrh`, Accessed: 2021-5-4.
33. R. Freund, W. Wilson and D. Mohr, *Statistical Methods* (Academic Press, Burlington, MA, USA, 2010).
34. I. Lobach, Statistical properties of undulator radiation: Classical and quantum effects, PhD thesis, The University of Chicago (2021).
35. I. Lobach, The source code for simulation of the longitudinal motion of a single electron in a storage ring `https://github.com/IharLobach/ursse`, (2020).
36. S.-Y. Lee, *Accelerator physics* (World Scientific Publishing, 2018).
37. H. Burkhardt, Monte Carlo generation of the energy spectrum of synchrotron radiation `http://cds.cern.ch/record/1038899/files/open-2007-018.pdf`, (2007).